Electronic surface states of liquid helium*†

Milton W. Cole‡

Physics Department, University of Washington, Seattle, Washington 98195

Electrons at the surface of liquid ^{4}He are potentially valuable probes of both static and dynamic properties of the interface. Two species of surface state are discussed. One of these is localized just above the interface, weakly bound by the image force. The existence of this state has been confirmed by direct spectroscopic observation. Measurements of parallel field mobility and lifetime on the surface are discussed and compared with predictions. The other surface state is an electron bubble held below the interface with an applied field. A resonance experiment in this geometry determines an effective mass different from the bulk liquid value. Studies of field emission from the bubbles lead to an evaluation of other bubble properties.

CONTENTS

I. INTRODUCTION

The behavior of extra electrons in liquid He has been extensively investigated during the last fifteen years. The subject has had particular appeal because of the superfluidity of ^{4}He and the applicability of Fermi liquid theory to ^{3}He at low temperatures. Certainly extra electrons will be used to study the superfluid phase(s) of ^{3}He at ultralow temperature.

One particularly exotic subject of this research is the electron "bubble," a cavity of $\sim$15 Å radius in which the electron resides. Because its size is intermediate between microscopic and macroscopic, the bubble exhibits behavior characteristic of both regimes, depending on the particular phenomenon under investigation. For the theorist, the self-consistent configuration of this system of N atoms plus one electron offers particular fascination and challenge.

Until recently, experiments with electrons at He surfaces were intended primarily to provide information about the bulk states. In particular, Sommer (So64a) found that the surface presented a barrier V_0 of more than 1 eV to electron transmission into the liquid. This represented an important element in the evolution of the bubble concept. Other experiments, of Careri *et al.* (CFG60) and Bruschi *et al.* (BMM 66), showed that in order to be ejected *from* the liquid, electrons had to overcome an energy barrier of order 25 Kelvin ($\approx$2.5 meV). Stimulated by these experiments as well as by more general aspects of the electron–He problem, Sommer, (64b), Cole, and Cohen (CC69, Co70b), and Shikin (Sh70, Sh71a, 71b) independently formulated descriptions of the electronic surface states for liquid He. This work has been considerably extended both theoretically and experimentally, although our understanding of several aspects remains incomplete. The present article will assess the "state of the art" in this area, emphasizing the basic concepts and their relation to those of other fields.

At the outset the reader must note a distinction between two species under discussion. The term "external" surface state refers to an electron outside (above) the liquid. The 1 eV barrier mentioned above inhibits penetration into the He. However, the image potential, given classically in terms of the static dielectric constant ϵ as a function of distance z from the surface by

$$V_{\text{image}}(z) = -Qe^2/z, \qquad z \geq 0, \tag{1}$$

$$Q = (\epsilon - 1)/4(\epsilon + 1), \tag{2}$$

attracts the electron to the liquid–vapor interface.[1] As a result, the wave function of the electron is localized near the interface, as depicted in Fig. (1). The electron is free to move parallel to the interface, but in so doing it is scattered by the liquid's excitations and the vapor. The energy spectrum, scattering properties, and mutual interactions of these "external" electrons are among the topics discussed in Sec. III.

The "internal" electron surface state, shown schematically in Fig. (2), is an electron bubble under the influence of an applied electric field which accelerates it toward the surface. In this case the image potential exerts an opposing force, directed into the buk liquid, tending to keep the electron in the medium. The net potential for the bubble has a shallow minimum 100–300 A below the surface. The oscillations of the bubble in this potential can be studied by resonance techniques (PW72) which yield effective mass and lifetime parameters somewhat different from values determined in bulk experiments. Another fruitful experimental approach is field emission from these states into the vacuum. The analysis of this situation is particularly intriguing because it convolutes the hydrodynamic (or kinetic) oscillatory motion of the bubble with quantum-mechanical tunnelling through the liquid above the bubble (SR73). This technique and others may be sufficiently sensitive to analyze some aspects of the structure and dynamics of the free liquid surface.

While almost all of the surface state experiments to date have used liquid ^{4}He, both internal and external states should also exist for liquid and solid hydrogen, neon and

* Research supported by the National Science Foundation.

† Based in part on an invited paper delivered at the 1973 San Diego meeting of the American Physical Society.

‡ Present address: Physics Department, Pennsylvania State University, University Park, Pennsylvania 16802.

[1] The implicit assumption of Eq. (2), that the vapor dielectric constant is unity, is valid to within one percent below 3 K. We note that the suggestion that the image potential plays a role in surface states was made by Shockley long ago (Sho39).

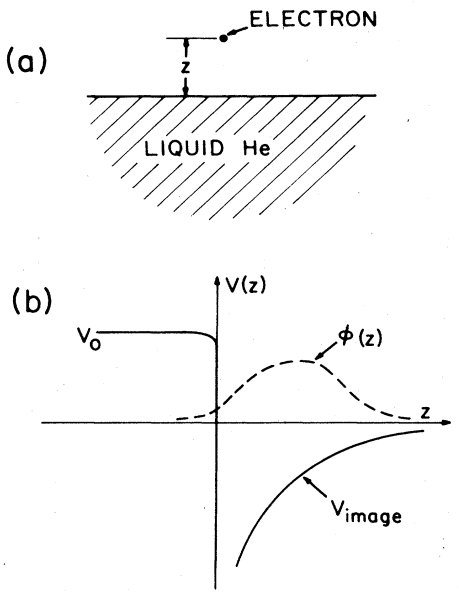

FIG. 1. (a) Geometry for external electron surface states. (b) Potential V and ground state wave function ϕ depicted schematically.

^{3}He (Co70b). These materials satisfy the sufficient condition of having a negative electron affinity (SJC68).[2] That is, the conduction band minimum lies above the vacuum level. Recently, Sak (Sa72) has extended this work to those ionic crystals (eg. LiF) which satisfy this criterion. Here the medium's electronic polarization is supplemented at low frequency by ionic polarization. The interaction with the electron proceeds via surface optical phonons which couple to the electron's motion, forming a surface polaron. Evans and Mills (EM72, EM73) have considered independently the more general case of electron localization due to surface polarization modes even if the electron affinity is positive.

Another analogous problem is that of positron surface states. If the (positron) work function ϕ_p is negative, as

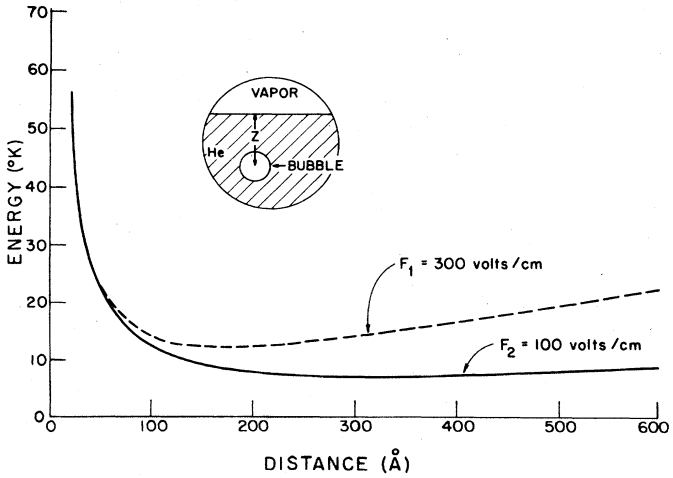

FIG. 2. Electrostatic energy of electron bubble as a function of distance below the interface for two different values of applied field. Inset shows geometry of bubble near surface.

[2] By comparison, this is a necessary condition for stability of the bubble.

may be the case for Al (CGHM73), such states definitely exist. In fact, they probably exist for a number of metals which have ϕ_p as large as +5 eV (HS73).

In this paper we shall discuss primarily the case of liquid ^{4}He, although it is clear that the concepts studied here have considerable application elsewhere in the physics of liquids and solids. However, the properties of the liquid ^{4}He surface make it a particularly useful medium to study. The time-average interfacial position of a liquid is uniformly flat, while it has structure for a solid. In contrast to the major problem of impurities at solid surfaces, for ^{4}He there is only one important impurity, ^{3}He, which actually localizes preferentially at the surface.[3] An additional feature of a liquid surface is its ease of deformation, which has been observed by Williams and Crandall (WC71a) for the external surface state on He. One particular merit of ^{4}He relative to

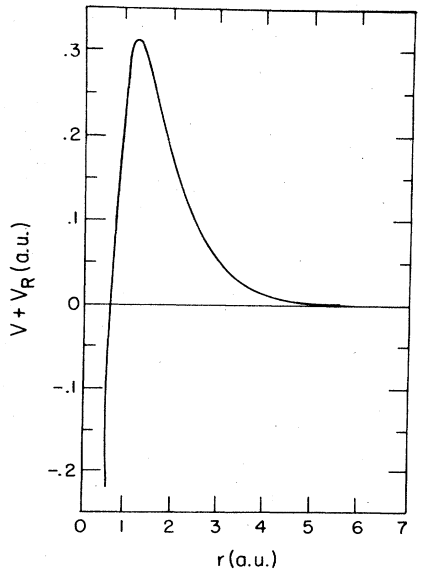

FIG. 3. The electron–He interaction $V + V_R$ as a function of separation. The attractive long-range tail is too small to discern. The apparent attraction at close approach is an artifact of the calculation. Units are Bohr radii and Hartrees (=2 Rydbergs). From (KJCR65).

other liquids is its temperature uniformity below the lambda point, which serves to eliminate disruptive boiling. A further advantage for the theorist is that the superfluid fraction is inviscid and irrotational, facilitating calculations of relevant liquid surface properties.

II. ELECTRON–HELIUM INTERACTION

It is important to understand how the electron–liquid interaction results from the electron–atom interaction. The need for this is obvious in a superficial sense because surface states are intermediate between free and bulk states. In any case we shall need to know specific parameters characterizing the electron's interaction in both limits of He density.

The result of a pseudopotential calculation by Kestner *et al.* (KJCR65) of the electron–He atom interaction is shown in Fig. (3). Because the exclusion principle requires

[3] This occurs because ^{3}He is lighter, so the zero-point energy is reduced (S71).

that the scattering electron wave function be orthogonal to the bound atomic states, there is a strong repulsion at small preparation r. This repulsion has a range comparable to the Hartree–Fock radius $\tilde{a}$ of He. At larger separation an attractive interaction becomes dominant, but the magnitude is too small for it to appear in Fig. (3). This weak attraction is entirely responsible for the states discussed here. The attractive tail of the potential derives from the force between the electron and the instantaneous dipole moment of the atom. In the adiabatic approximation, valid for frequencies small compared to $\delta E_{12}/\hbar$, where δE_{12} is the first atomic excitation energy, the moment is proportional to the polarizability α. In this limit the interaction is of the form

$$V_{\rm pol}(r) = -\alpha e^2/2r^4, \qquad r \gg \tilde{a}. \tag{3}$$

The net e–He interaction in the limit of zero energy is represented by the scattering length a_s, related to the electron–atom cross section $\sigma = 4\pi a_s^2$. The sign of a_s is determined by the competition between the repulsive core and attractive tail of the interaction. Helium has the smallest polarizability and the largest δE_{12} of any atom. Consequently, its scattering length is relatively large and positive. The trend in the noble gases toward softening core and increasing α is exhibited in Table I, which also shows the consequent variation in a_s.

The key parameter characterizing the electron–liquid interaction is V_0, the conduction band minimum energy. At first glance one might question the existence of a band structure with well defined eigenvalues for an electron in a liquid. It has been argued (Ll67, Zi67), however, that when the electron wave-vector k is near zero for He or other noble gases, the states are insensitive to medium structure. Thus one can calculate V_0 for a crystal having the liquid's density. This approach was used by Burdick (Bu65) to obtain $V_0 = 1.09$ eV, in good agreement with 1.04 eV obtained by Jortner *et al.* (JKRC65) using the Wigner–Seitz model, which is by assumption structurally insensitive. More recently, Fetter (Fe74) and Tankersley (Ta73) have derived a diagrammatic expansion for V_0 which makes explicit reference to two-particle correlations via the liquid structure factor. The V_0 that results is 0.97eV at $T = 0$, but the expansion may be inadequate at liquid density, since the second term is almost half of the leading term (the optical potential),

$$V_{\rm opt}(n) = 2\pi n a_s \hbar^2/m, \tag{4}$$

where n is the liquid number density, which depends weakly on T.

TABLE I. Polarizability α, atomic radius $\tilde{a}$, and scattering length a_s for several atoms and H_2. The values of α and a_s are experimental; all quantities are taken from (JK70). For H_2, the α shown is an average of the diagonal elements of the polarizability tensor.

	α(Å^3)	$\tilde{a}$(Å)	a_s(Å)
He	0.20	0.75	0.61
Ne	0.39	0.56	0.21
Ar	1.65	0.79	−0.90
H_2	0.79	1.00	0.74

These theoretical estimates compare favorably with experimental values of (1.3 ± 0.3), $(1.02 \pm .08)$, 0.95 and 0.82 eV found by Sommer (So64a) via electron injection, Woolf and Rayfield (WR65) with photoinjection, Zipfel and Sanders (ZS68; see also MD70) with photoejection from bubbles, and Schoepe and Rayfield (SR73) with tunneling from electronic surface states, respectively. These experiments were performed at finite T, but n is the principal determinant of V_0.

It should be noted that the processes described by these calculations and studied experimentally are adiabatic. The small electron/atom mass ratio guarantees the validity of this assumption for a short time ($\approx 10^{-11}$–10^{-12} sec) during which the liquid cannot deform in response to the electron. Eventually the liquid must respond to the electron because of the instability of the delocalized Bloch-like state with respect to bubble formation.

III. EXTERNAL SURFACE STATES

A picture of the external surface state follows from our description of the electron–He interaction. The barrier V_0 prevents significant electron penetration into the medium, as long as the adiabatic approximation remains valid. The potential energy $V(z)$ of the electron far above the surface, say $z > b$, will have the classical electrostatic form [Eq. (1)]. Closer to the surface, the potential will be modified because of the atomicity of the liquid, the lack of definition of the interface $z = 0$, and the incomplete response of the dielectric polarization to a high-frequency field. The last of these is negligible for He because of the high characteristic frequencies of the atomic electrons, $\omega_c \approx \delta E_{12}/\hbar \approx 3 \times 10^{16}$ sec^{-1}. Specifically, an estimated frequency of the perturbing electron's field,

$$\omega_e \approx \dot{z}/z \approx (|\, V(z)\,|/m)^{1/2} z^{-1},$$

becomes comparable to ω_c only when the electron is within 1 A of the surface. The dot denotes a time derivative.

While we are unable to improve significantly upon the deficiency of the classical potential due to microscopic structure of the surface, this turns out to be no serious problem because of the small amplitude of the wave function for small z. Spontaneous thermal fluctuations of the liquid surface, which have amplitude comparable to an interatomic spacing are unimportant for the same reason (Co70a). However the static and dynamic oscillations of the surface *due* to the electron deserve separate treatment for the mobility problem (Sec. C).

With these limitations in mind, we write the potential for the wave function ψ in the effective mass approximation

$$V(z) = V_0, \qquad z < 0 \tag{5a}$$

$$= -Qe^2/b, \qquad 0 < z < b \tag{5b}$$

$$= -Qe^2/z, \qquad z > b. \tag{5c}$$

The quantity Q, defined in Eq. (2), depends on temperature T through the dielectric constant of the liquid and negligibly on that of the vapor, until one gets to relatively high T. The similarity of Eq. (5c) to the Coulomb potential suggests the notation Q, where Qe is the image charge. At $T = 0$,

Q for He is about 7×10^{-3}, corresponding to a rather weak attraction.

Somewhat arbitrary choices of Eq. (5) include the surface plane $z = 0$ as the image plane, and the constant b, for which we use the He interatomic spacing, 3.6 Å. Experimental precision is now sufficient to test these values. A more drastic approximation at first glance is to neglect the image potential when the electron is inside the medium. This omission is acceptable because V_0 is so large relative to this and all other characteristic energies in the problem that the correction is negligible.

Due to the invariance of the liquid with respect to horizontal translation, the eigenfunctions and eigenvalues of the Hamiltonian of Eq. (5) are of the form

$$\psi_k(\mathbf{r}) = A^{-1/2} \exp(i\mathbf{k}\cdot\zeta)\phi(z), \tag{6}$$

$$E_k = E_\perp + \hbar^2 k^2/2m. \tag{7}$$

Here A is the surface area, $\mathbf{k}$ the wave vector, ζ the component of $\mathbf{r}$ parallel to the surface, and z the perpendicular component of $\mathbf{r}$. For states near the conduction band minimum in He the effective mass equals the bare electron mass m, as follows from the effective mass sum rule. Thus the boundary conditions on ψ, the envelope function in the effective mass approximation, reduce to those on an ordinary wave function—continuity of ψ and its derivative (BD66, BD67). The Schrödinger equations for perpendicular motion are

$$\phi'' - \gamma^2\phi = 0, \qquad z < 0 \tag{8a}$$

$$\phi'' + (2m/\hbar^2)(E_\perp + Qe^2/b)\phi = 0, \qquad 0 < z < b \tag{8b}$$

$$\phi'' + (2m/\hbar^2)(E_\perp + Qe^2/z)\phi = 0, \qquad z > b \tag{8c}$$

where the prime denotes differentiation with respect to z and

$$\gamma^2 = (2m/\hbar^2)(V_0 - E_\perp).$$

The other condition on ϕ is that it vanish as $|z| \to \infty$. The solution of Eq. (8a) in the liquid is a decaying exponential with a characteristic decay length $\gamma^{-1} \approx 2.5$ Å. In the intermediate region ϕ is an oscillatory function with much longer wave length ($\approx$100 Å). The solution for $z > b$ is the Whittaker function (WW63), a form of confluent hypergeometric function:

$$\phi_l(z) = W_{l,1/2}(2Qz/la_0), \tag{9}$$

where l is a quantum number related to the energy by

$$E_{\perp l} = -(Q^2/l^2)R_0. \tag{10}$$

Here $R_0 = e^2/2a_0$ is the Rydberg constant, and a_0 is the Bohr radius. Cole (Co70b) has studied the properties of these eigenfunctions in some detail. The essential result is that the small magnitude of Q for He results in a binding energy which is of the order of one per cent of V_0. The problem therefore reduces approximately to the solution of Eq. (8c) with the boundary condition that ϕ vanish at the origin. This, however, is identical to the radial Schrödinger equation for r times the s-state wave function for a Coulomb potential due to a charge Qe at the origin. The spectrum in this limit is exactly Eq. (10) with integral l, and the wave functions are products of an exponential and an associated Laguerre polynomial. For example, the energy and normalized wave function of the ground state are

$$E_{\perp,1} = -Q^2R_0 \approx -0.65 \text{ meV} \approx -7.5 \text{ Kelvin}, \tag{11a}$$

$$\phi_1 = 2a^{-3/2}z \exp(-z/a), \tag{11b}$$

$$a = a_0/Q. \tag{11c}$$

The Bohr radius for this state (i.e., point of maximum probability density) is $a \approx 76$ Å from the surface; the expectation value of z is 3/2 this value, or 114 Å. We can now understand why the properties are insensitive to the rather crude approximations used earlier. The electron is most likely to be found a distance of about 20 times the interparticle spacing from the surface. Its wave function becomes small within a few angstroms of the interface. The binding energy is infinitesimal on the scale of V_0 ($\approx$1 eV), but fortunately large enough to have some probability of being bound at typical experimental temperatures. The observe aspect of these factors is that the external surface state of He will not provide a sensitive probe of the liquid's surface properties.

In later sections of this paper, we shall use for simplicity the eigenfunctions of the pure Coulomb problem, which corresponds to infinite V_0. Quantities characterizing the accuracy of this approximation include the penetration fraction of the electron into the medium,

$$R_p^{(n)} = \int_{-\infty}^{0} \phi_n^2(z)\, dz \Big/ \int_{-\infty}^{\infty} \phi_n^2(z)\, dz,$$

and δl, defined as the increase in l required to bring it to the integer value n. Calculations of Cole (Co70b) using the true wave function show that $R_p^{(1)} = 1.2 \times 10^{-4}$ and $\delta l = 0.046$ for the ground state on He. These quantities are considerably larger for other systems, so our approximation will be accurate only in the He case. One important point concerning δl is that it is nearly independent of energy, analogous to the quantum defect in atomic physics.

Using the calculated value of δl and $Q = 6.95 \times 10^{-3}$ in Eq. (10), the first excitation energy is $E_{12} = 5.50 \times 10^{-4}$ eV, compared with 4.94×10^{-4} eV for $\delta l = 0$ (i.e., $V_0 = \infty$). A measure of the sensitivity of this result to the value of V_0 comes from differentiating Eq. (10),

$$\partial E_l/\partial V_0 = +(2Q^2R_0/l^3)\partial l/\partial V_0.$$

Since $\partial l/\partial V_0$ is approximately independent of l, it can be evaluated from the ground state result $R_p^{(1)}$, yielding

$$\partial E/\partial V_0 = l^{-3}R_p^{(1)}.$$

Recently Grimes and Brown have performed an extremely precise microwave absorption experiment which confirms the existence of image potential induced surface states (GB74). Microwave radiation of frequency $\nu > 125$ GHz is absorbed by the surface electrons at one or more values of an electric field F normal to the surface. Varying F shifts the levels linearly and the resonance ν value shifts

accordingly [Figs. (4) and (5)]. A zero field extrapolation gives the unperturbed transition frequencies $\nu_{12} = 125.9 \pm 2$ GHz, and $\nu_{13} = 148.6 \pm 3$ GHz. The "hydrogenic limit" $V_0 = \infty$ with a cutoff $b = 0$ predicts 119.3 and 141.3 GHz, respectively. The more realistic model $V_0 = 1.3$ eV and $b = 3.6$ Å (an interatomic spacing in the liquid) yields 133.1 and 156.5 GHz, respectively. Both values fall on the high side of experiment. Using the perturbation approach mentioned above, one finds that $V_0 = 1.58$ eV fits both absorption lines. This is rather high compared with previous values discussed in Sec. II, so the calculations should be repeated to determine a reasonable pair V_0 and b which fits the data. {*Note added in proof:* H.-M. Huang, Y. M. Shih, and C.-W. Woo [J. Low Temp. Phys. **14**, 413 (1974)] recently calculated eigenvalues $-9K$, $-2K$ from a more realistic surface density profile. The corresponding transition frequency, $\nu_{12} = 146$ GHz, is high, perhaps because of their use of the optical potential, Eq. (4), instead of V_0 in the liquid.}

A further point of agreement with the model is the Stark

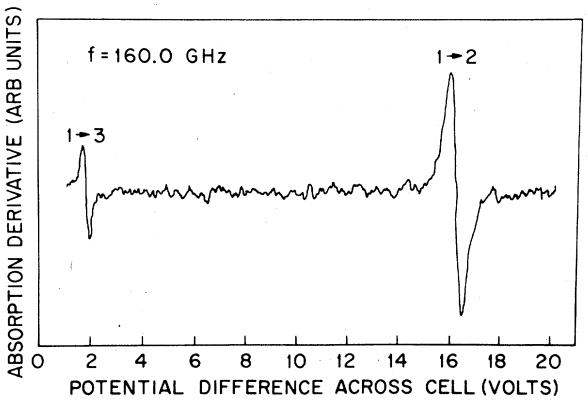

FIG. 4. Derivative absorption curves of external surface electrons as a function of potential difference across the interface, at $T = 1.2$ K. The first two absorption lines are seen. From (GB73).

shifts of the absorption lines with field

$$d\nu_{ij}/dF = e(\langle z\rangle_i - \langle z\rangle_j)/h.$$

A calculation using hydrogenic wave functions gives 0.8 GHz/(V/cm) and 2.1 GHz/(V/cm), respectively. Because of uncertainty in the magnitude of F, Grimes and Brown were able to obtain only the ratio of this derivative for the two transitions, and found a value 2.6 ± 0.2 compared with a predicted 2.67. Finally, the intensity ratio of the $1 \rightarrow 2$ transition to the $1 \rightarrow 3$ is observed to be about 5, compared with the ratio of oscillator strengths $8^6/3^{10} \approx 4.4$.

A. Distribution at finite temperature

For each band l of perpendicular motion, the two-dimensional free-particle motion of the electron parallel to the surface gives rise to a density of states per unit area $N_l(E)$ which is constant above the threshold $E_{\perp l}$

$$N_l(E) = (m/\pi\hbar^2)\theta(E - E_{\perp l}), \tag{12}$$

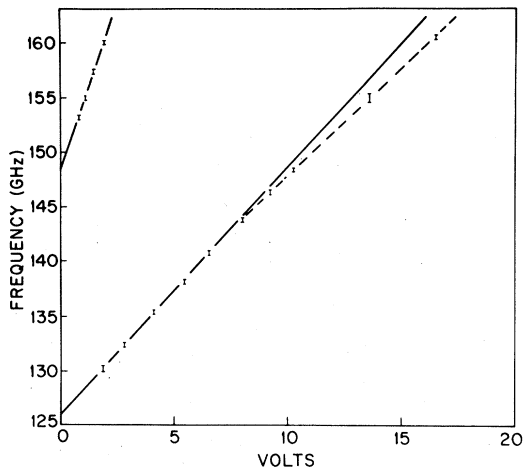

FIG. 5. Potential difference at resonance as a function of radiation frequency. The lower set of points refers to the $1 \rightarrow 3$ transition, and the upper set to $1 \rightarrow 2$. The solid line corresponds to a linear Stark effect which extrapolates to the zero field, unperturbed absorption frequencies. The dashed curve, drawn to aid the eye, implies some quadratic dependence. From (GB74).

including spin degeneracy. Here θ is the usual step function. The total density of states $N(E)$ is then simply $(m/\pi\hbar^2)$ times the number of states of perpendicular motion which have $E_\perp < E$. This result, shown in Fig. 6, has a discontinuity at each eigenvalue $E_{\perp l}$ because the lth perpendicular state contributes only above that energy. Thus for $E < 0$,

$$N(E) = (m/\pi\hbar^2) \times \text{integral part of } (-R_0Q^2/E)^{1/2},$$

which diverges near zero energy because the perpendicular level spacing tends to zero with increasing quantum number as l^{-3}.

One consequence of this large density of weakly bound states is that entropy considerations result in their dominating the thermal distribution of occupied states at finite temperature T (CW72). In fact these states' contribution

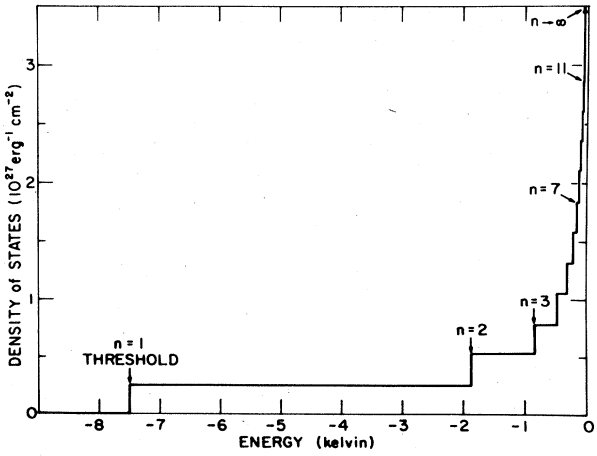

FIG. 6. The density of states $N(E)$ for the external electronic surface states. A step occurs at each eigenvalue of perpendicular motion. For large quantum numbers and in the continuum, $N(E)$ lies far off scale.

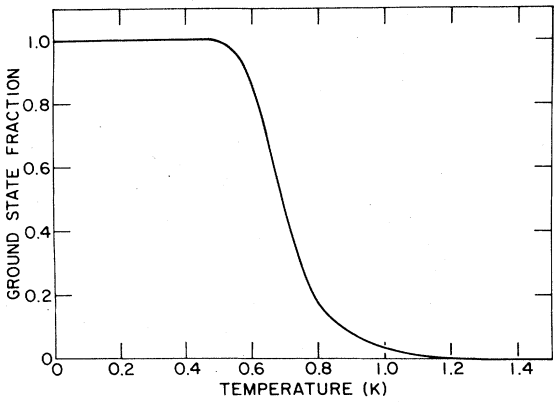

FIG. 7. The fraction of electrons in the ground state of perpendicular motion as a function of temperature, in the absence of an applied field.

to the partition function

$$Z = \sum_n \exp(-\beta E_n),$$

$$\beta^{-1} = k_B T,$$

is divergent, because of the infinite density of states near zero energy. The problem is analogous to one treated by Fermi (F24) for the H atom, differing only in the absence of an n^2 degeneracy factor. One realizes that the divergent contribution of large n states is unphysical because the wave functions of these states extend far from the surface, where the assumed z^{-1} potential is inaccurate. In particular, vapor atoms or walls modify the potential. A simple Ansatz is to place a "wall" (infinite barrier) a distance L from the surface, where L might be of order an electron mean free path, or an experimental chamber dimension. We shall assume $L = 1$ cm, but the results are relatively insensitive to this assumption.

The new spectrum of perpendicular states will differ little from Eq. (10) apart from elimination of the divergence. Those discrete states which have an outer classical turning point at $z < L$ will not be greatly affected by the presence of the wall. These have $E < -Qe^2/L$ ($\approx -10^{-5}$ K) and quantum numbers $n < N_{\max} = (L/2a)^{1/2} \approx 850$. Near zero energy ($|E| < Qe^2/L$) the WKB approximation can be used to estimate the level spacing. The nth state satisfies

$$(n + 1/2)\pi = \int_0^L k(z, E)\, dz,$$

$$k^2(z, E) = 2m(E - V(z))/\hbar^2. \tag{13}$$

One derives the level spacing δE from taking differences of Eq. (13):

$$\pi(\delta E)^{-1} = (m/2\hbar^2)^{1/2} \int_0^L dz\, (E + Qe^2/z)^{-1/2}.$$

For the special case $E = 0$ this yields

$$(\delta E)^{-1} = (3\pi)^{-1}(2mL^3/\hbar^2 Qe^2)^{1/2}, \tag{14}$$

which differs by a factor $4/3\pi$ from $(\delta E)^{-1}$ for the discrete spectrum at $n = N_{\max}$. The density of quasicontinuum states having $E_\perp > Qe^2/L$ can be approximated by that of free particles in a box,

$$\nu_\perp(E) = L(m/(2\pi^2\hbar^2 E))^{1/2}. \tag{15}$$

With this form for $\nu_\perp(E)$, the equilibrium ratio at temperature T of ground state to continuum state populations is

$$N_1/N_c = \hbar L^{-1} \exp(\beta E_{\perp 1})\, (8\pi\beta/m)^{1/2}.$$

As shown in Fig. (7), the fraction of electrons in the ground state drops rapidly from unity to nearly zero between 0.5 K and 1 K. Essentially all of the bound electrons are in the ground state below 1 K, so in this regime the approximate treatment of the excited states is adequate.

To facilitate study of the bound states at $T > 1$ K, experimentalists have applied an electric field oriented so as to hold the electrons near the surface. This certainly modifies the highly excited states, but the lowest states may be only weakly affected. As a borderline example, a field F of order 100 V/cm shifts the $n = 1$ state upward by Fe $\langle z\rangle \approx 1.3$ K and changes the $1 \rightarrow 2$ transition energy by Fe $(\langle z\rangle_2 - \langle z\rangle_1)$ to a value of 9.6 K from a zero field value of 5.7 K. In any case, the applied field eliminates the high density of continuum states and thus reduces their population. We can estimate this effect with the help of a number of assumptions. First we take the total potential to be simply a sum of image and field contributions, $V_1 \approx -Qe^2/z + Fez$. This potential has no analytic solution, so we resort to an approximation which yields a reasonable estimate for the density of states, if not the actual eigenvalues. Specifically we choose a simple, qualitatively similar potential $V_2(z)$,

$$V_2(z) \equiv -\bar{V} + Fez,$$

$$\bar{V} \equiv Qe^2/z_a \equiv Fez_a.$$

The eigenfunctions of the Schrödinger equation with V_2 are Airy functions, and the eigenvalues (An65) are

$$E_i = -\bar{V} + |\alpha_j|\, (e^2F^2\hbar^2/2m)^{1/3}$$

where α_j is the jth zero of the Airy function. Using the asymptotic limiting form $\alpha_j \sim -(3\pi j/2)^{2/3}$, one can derive a density of states for perpendicular motion (including spin)

$$\nu_\perp(E) \sim (8m(E + \bar{V}))^{1/2}/(\hbar\pi eF).$$

This in turn generates a partition function

$$Z_F = \int_{-\bar{V}}^{\infty} dE\, \nu_\perp(E) \exp(-\beta E)$$

$$Z_F \cong (2m/(\pi\beta^3))^{1/2}(\hbar eF)^{-1} \exp(\beta\bar{V}). \tag{16}$$

This represents a moderately accurate estimate of the contribution to Z of the large eigenvalues of V_1. Typical values of $F \approx$ (10–100) V/cm yield a Z_F of order unity.[4] In contrast, the contribution to the total partition function from the ground state, at energy $-E_{\perp 1} + Fe\langle z\rangle_1$, is much

[4] The small F divergence in Eq. (16) is spurious, as one must proceed to box quantization in this limit.

greater than this. Thus the field, even if quite small, effectively depopulates the highly excited states.

B. Electron–electron interaction

An important element of the problem that has been neglected thus far is the Coulomb repulsion between electrons. If N electrons are assumed to be well localized in the z direction and uniformly distributed over a circle of diameter D in the surface plane, the electrostatic energy per electron is of order Ne^2/D. The system becomes unbound when this is comparable to the assumed binding energy, Q^2R_0, or equivalently when

$$N \approx \tfrac{1}{2}Q^2D/a_0,$$

which is of order 5000 for $D = 1$ cm. This represents a serious constraint to which all experiments so far have accommodated by modifying the geometry. One approach is to apply an external field, but this complicates analysis considerably. The potential depends on the applied field and the number of electrons present, determined by the length of time the source (radioactive or corona discharge) was on. These electronic states may bear little resemblance to the single particle states discussed above. An alternative is to study the surface states of electrons above an adsorbed He film. Calculations by the author (Co71) for the case of a metallic substrate indicate that a binding energy of order 0.03 eV results for a 50 Å film, an enhancement factor of almost 50 times the bulk liquid result. A complicating aspect of the film geometry is the possibility of tunneling through the He if the film is thin.

One of the most intriguing hypotheses proposed for both internal and external surface electrons is that they may form a two-dimensional Wigner crystal. The argument, due to Crandall and Williams (CW71, Cr73), notes that at low electron density the potential energy of Coulomb repulsion dominates the kinetic energy. Hence at sufficiently low T an ordered state which minimizes the potential energy will be stable relative to a disordered one.

As mentioned previously, most experiments require an applied electric field to overcome Coulomb interactions. Here such a field, due typically to a submerged positive electrode, plays the role of the positive background usually required for charge neutrality. Characteristic dimensions in the experiments of Williams, Crandall, and Willis (WCW71, CW72) are such that the interelectronic spacing (10^4 Å) is much larger than the z-wise spread in the charge density[5] and the Bohr radius, but much smaller than the electrode dimension. Thus lateral edge effects are probably unimportant. The system is essentially two-dimensional with respect to long wavelength behavior, although nonplanar correlations may be important at shorter wavelengths.

Assuming a square array for the electrons, Crandall calculated the excitation spectrum for the case of a one-micron lattice constant. The spectrum has two branches, a transverse acoustic branch and a longitudinal plasmonlike branch which has $\omega \propto q^{1/2}$ at long wavelengths.[6] The unusual q dependence occurs because the two-dimensional Fourier transform of the Coulomb potential varies as q^{-1} (Cr72, Ch71). With the phonon spectrum, one can calculate the fluctuations $\langle r^2 \rangle$ of electrons about their assumed equilibrium positions. Taking into account the long wavelength cutoff in the spectrum due to finite lateral size, one finds (Cr73)

$$\langle r^2 \rangle \approx (2 \times 10^{-11} + 3 \times 10^{-10}T) \text{ cm}^2,$$

so that the root mean square fluctuation at 1 K, for example, is of order one-sixth of the lattice constant. Thus anharmonic corrections are relatively unimportant.

Recently considerable attention has been focused on the nature of solids in two dimensions (DB72, KT73, ElG73). Although no truly long-range positional order is present at finite T in two dimensions, angular correlations do have infinite range (Me68). Kosterlitz and Thouless have described melting in terms of an instability of the system with respect to dislocation formation. A true phase transition is predicted to occur. An estimate of the melting temperature assuming an acoustic excitation spectrum is (ElG73)

$$T_m = mk_B\theta_D^2/(32\pi^2\hbar^2 n),$$

where n is the density, and θ_D the Debye temperature. This is a qualitative estimate because of the invalid assumption of acoustic behavior. Simply assuming a Debye spectrum and taking Crandall's calculated value for the speed of sound, one obtains a melting temperature of 4.5 K for $n = 10^8$ cm^{-2}.

The experimental evidence concerning the existence of an ordered state on the surface is inconclusive. A diffraction experiment could provide a direct test of the electronic arrangement; while no delta functions are present in the structure factor at finite temperature, very sharp peaks should appear because of short-range order (MS70). More indirect verification could follow from mobility and lifetime measurements, which we discuss below. We emphasize that the most important calculation remains to be done. That is a comparison of free energies of the ordered and disordered states in order to determine the phase diagram.

C. Surface state lifetime and mobility

Williams, Crandall and Willis have studied the lifetime of electrons on the surface of liquid He (WCW71, CW72) in the temperature range 1.1–3.5 K. Electrons deposited above the surface by a negative corona discharge are held there with the help of an electric field due to electrodes above and below the interface. As the upper electrode oscillates vertically, its charge variation probes the surface potential. The experiment measures the decay of surface electronic charge after the holding field is removed or reversed. For short times, this decay is exponential with a characteristic time τ of order 10^{-4} sec. This result disagrees with that obtained with a different technique by Ostermeier and Schwarz (OS72), discussed below.

Crandall (Cr74) has calculated τ by considering the electrons' interaction with vapor atoms and ripplons

[5] This will be the case if less than the maximum possible charge density is adsorbed, so that the field remains nonzero far from the surface.

[6] Both polarization and propagation vectors of these modes are in the surface plane.

(quantized oscillatory modes of the liquid surface). These processes can cause "vertical" transitions between different perpendicular states at the expense of energy of parallel motion.[7] Evaporation transitions, from ground state to continuum, each deplete the surface by the binding energy per electron. However, the condensation process is unlikely because the applied field draws continuum electrons away. Consequently, the characteristic temperature of the electron system is below ambient and the activation temperature $|E_1|/k_B$ does not enter τ explicitly, except at low temperature when the cooling effect becomes negligible.

The lifetime so obtained is shorter than that found experimentally by Williams *et al.* The discrepancy may result from the applied field and space charge. An alternative speculation (Cr74) is that the electrons are Wigner-crystallized, although we have no lifetime prediction for this configuration to compare with experiment.

Predictions of the mobility of electrons with respect to motion parallel to the surface have been made by Cole (Co70b). Scattering by vapor atoms and ripplons limits the mobility in a manner analogous to impurity and phonon scattering of electrons in solids. One calculates a momentum transfer rate (inverse relaxation time) due to the electron–ripplon interaction,

$$\lambda_r = \lambda_{r0}/(\beta E_{||}),$$
$$\lambda_{r0} = \pi^2 Q^4 n_l^2 \alpha^2 m^4 e^{12}/4\hbar^9\sigma, \qquad E_{||} = \hbar^2k^2/2m, \tag{17}$$

for transitions in which the perpendicular ground state is unchanged. The liquid surface tension σ and the number and mass densities, n_l and ρ, enter through the ripplon dispersion relation,

$$\omega^2 = \sigma q^3/\rho, \tag{18}$$

and the interaction matrix element.[8] The rate (17) has a plausible dependence on effective charge Q in that a large value corresponds to close electron proximity to the surface and frequent scattering by surface oscillations.[9]

One can calculate the momentum transfer rate λ_V due to vapor atom scattering using a contact pseudopotential e–He atom interaction and a method of Duke (Du68) to treat the anisotropic scattering geometry. The result is

$$\lambda_V = 3\pi^2 n_V a_s^2 \hbar/2ma, \tag{19}$$

where the vapor density n_V varies rapidly with temperature. This expression assumes the electron to be in the ground state of perpendicular motion, a valid approximation if the charge density is small and either T is low or a holding field is present. The total scattering rate λ, the sum of λ_r and λ_v, can be used to derive the two-dimensional mobility[10]

$$\mu(T) = (e/m)\int_0^\infty dk k^3 \lambda^{-1}(T,k) \times \exp(-\beta E_{||}) \Big/ \int_0^\infty dk k^3 \exp -(\beta E_{||}),$$
$$\mu(T) = \mu_V(T)[1 + c^2 e^c E_1(c) - c], \tag{20}$$

where $\mu_V(T)$ is a mobility calculated by including only vapor atom scattering, E_1 is an exponential integral (GR65, p. 312), and $c = \lambda_{r0}/\lambda_V(T)$ is the ratio of ripplon to vapor atom scattering rates for thermal electrons.

At low temperature (<1 K) ripplon scattering becomes dominant, since n_V becomes exponentially small.[11] Because of the particular dependence $\lambda_r^{-1}\alpha\lambda\ \beta E_{||}$ in Eq. (17), the mobility asymptotically approaches a constant value in this regime. This behavior of μ, depicted in Fig. 8, is a critical test of the ripplon model (Co70b).

The character of the electron motion must change at high He vapor density from propagation with occasional scattering to localization in protobubbles, a transition observed in bulk He vapor near $n_V \approx 10^{21}$ cm^{-3}, or $T = 3.5$ K (LS67, EC70, 71, He73). Certainly this is an extreme upper limit for the validity of the calculation, since by taking the states to be T independent we neglect variation in both V_0 and n_V, and this multiple scattering regime is poorly described by Eq. (19).

Several rather ingenious techniques have been devised to

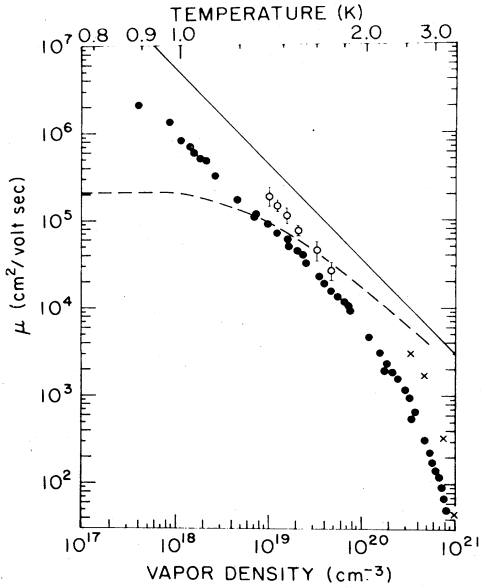

FIG. 8. The temperature-dependent mobility of an external surface state electron moving parallel to the surface. The theory (dashed line) includes both ripplon and gas atom scattering (Co70b). Open circles are data of (BG72); solid circles from (ST71). The solid line and crosses are theory and experiment, respectively, in three-dimensional vapor (M46, LS67).

[7] A single scattering event transfers little energy to or from an electron because of the latter's small mass.

[8] The gravitational term omitted from Eq. (18) contributes only for wavelengths longer than 0.1 cm.

[9] The ripplon scattering result of (Sh71a and 71b) is incorrect unless an applied field $F \gtrsim 10^3$V/cm is present.

[10] Equation (20) corrects a numerical error in (Co70b).

[11] This situation is the reverse of the familiar case of resistivity in solids, which at low T is determined by impurity scattering rather than phonons.

measure this surface mobility. Sommer and Tanner (ST71) employed a set of three submerged electrodes and one vapor electrode which create a vertical holding field. A voltage pulse applied to one submerged electrode is transmitted via the surface charge to another electrode. The relative phase of input and output signals is related to the energy dissipation in the surface layer, from which the electron mobility is deduced.[12] The values obtained, shown in Fig. 8, fall below single vapor atom scattering theory (M46) and experiment (LS67) for three dimensions. However the data do not show the low T limiting value predicted by the ripplon scattering calculation. If few of the electrons are in the ground state this would be expected, since the ripplon matrix element falls off rapidly with z. This possible resolution of the discrepancy remains uncertain.

Ostermeier and Schwarz (OS72) subsequently measured the parallel mobility directly. Their time-of-flight method has the advantage of using small surface charge density (5×10^5 cm^{-2}) and is capable of discriminating a distribution of mobility values, if present. The data, however, indicated a unique value of the mobility, equivalent to the three-dimensional result of Levine and Sanders. In addition this experiment measured an upper limit of 10^{-5} sec for the lifetime, in disagreement with the previous results of Williams, Crandall and Willis (WCW71, CW72). A possible origin of these differences is the absence of a large holding field in the Ostermeier–Schwarz experiment, which would be required to significantly populate the ground state (see Fig. 7) in this temperature range ($T > 1.06$ K). These experiments are being extended to lower T in the hope of seeing evidence for ripplon scattering (073).

The most recent determination of the surface mobility is the cyclotron resonance experiment of Brown and Grimes (BG72). Their microwave cavity has a resonant frequency of 2.35×10^{10} Hz in the TE_{111} mode. A DC magnetic field $H_0 = 8.3$ kOe oriented perpendicular to the surface is resonant if the cyclotron mass equals the bare mass, as was found to be the case within experimental error. The linewidth of the absorption signal gives the scattering rate, and mobility. The results, shown in Fig. 8, agrees qualitatively with the calculation, but does not extend to sufficiently low T to test for ripplon scattering.

The two-dimensional character of the states is demonstrated by the data shown in Fig. 9. If the field is tilted at an angle θ with respect to the surface normal, its magnitude must be increased to $H_0 \sec\theta$ to keep the perpendicular component constant, since it is the surface-parallel motion which is quantized. The question of whether the image potential or holding electric field is dominant in the binding to the surface was resolved in favor of the former because of insensibility of the absorption line shape and position to applied field (BG72).

Gor'kov and Chernikova recently showed that cyclotron resonance can detect a Wigner-crystallized state (GC73). The resonance frequency in such a state is calculated to be $(\omega_c^2 + \tilde{\omega}^2)^{1/2}$, where ω_c is the bare frequency, and $m\tilde{\omega}^2 r^2/2$ is the single particle potential of an electron about its equilibrium position. For the density of the Brown–Grimes experiment ($n \approx 5 \times 10^8$ cm^{-2}), $\tilde{\omega} \approx 10^{11}$ Hz $> \omega_c \approx$

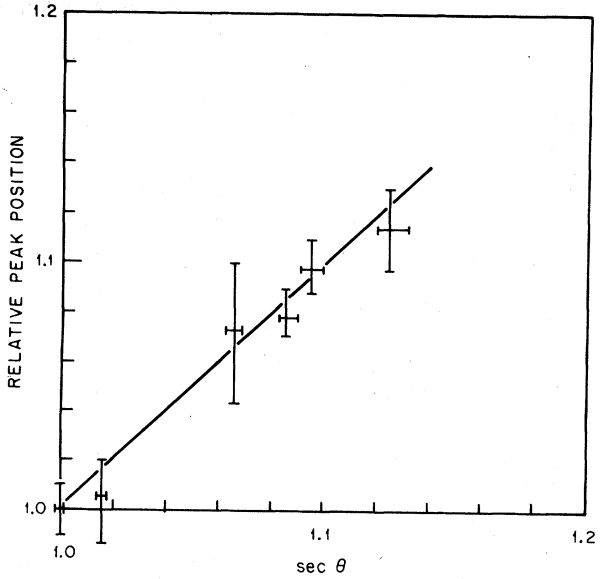

FIG. 9. Tilt angle (θ) dependence of $H(\theta)$, the magnetic field which gives maximum absorption in the cyclotron resonance experiment of Brown and Grimes (BG72), measured relative to $H(0)$. The 45 degree line corresponds to strictly two-dimensional motion.

2×10^{10} Hz so the resonance frequency should have differed from ω_c; this was not observed. One possible explanation for the discrepancy is that the lattice melting temperature T_m is lower than the lowest temperature studied, 1.3 K. This is not unreasonable in view of the crudeness of the estimate $T_m \approx 4.5$ K in the preceding section.

An alternative hypothesis is that the strong interelectronic interaction responsible for creation of the lattice necessitates a many-body treatment of its coupling to the magnetic field, which has not been provided.

D. Surface deformation and electron localization

Thus far we have assumed the liquid surface to be perfectly flat, apart from consideration of ripplons and their interaction with electrons. However, this assumption is inconsistent with the existence of the force $(-dV/dz)$ on the electron due to the liquid. It follows from Ehrenfest's theorem that the net force on the liquid due to the electron is zero. This force is not distributed uniformly, of course, since it consists of a contact interaction at the $z = 0$ plane, plus the long range electrostatic force [see Eq. (5)]. It is reasonable to inquire, therefore, how the liquid responds to the external field of the electron. A related question is whether there exists a localized state of a single electron above a deformed surface.[13] It is obvious that a vertical applied field F will cause such localization, and Williams and Crandall (WC71a) have observed a depressed surface for the case of high electron density (see Fig. 10). Shikin (71a, 71b) has studied localization of a single electron, finding the lateral extent and binding energy of such a state

[12] Non-ohmic effects, present if the signal amplitude was greater than 0.2 V, have been discussed by Crandall (Cr72).

[13] Quite generally, the electron will be dressed by ripplons. We describe here the special case of an electron moving above a static distortion, a valid solution in the limit of electronic frequency much higher than medium frequencies.

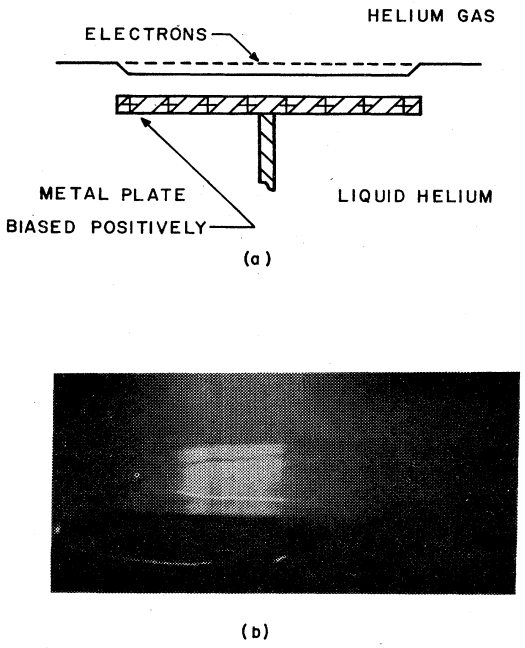

FIG. 10. Depression of a liquid He surface due to the presence of 2.5×10 electrons/cm^2. The applied field is 2000 V/cm. The depth of the depression is about 0.1 mm. From (WC71a).

to be

$$A_l = \pi\sigma a^3/(eF),$$

$$E_b \approx \hbar^2/(2mA_l), \tag{21}$$

which give $A_l \approx 10^{-9}$ cm^2, and $E_b/k_B \approx 10^{-2}$ K if $F = 300$ V/cm. It would be interesting to see whether a variational calculation yields a higher value of E_b. Equally desirable are estimates and measurements of the effective mass, which is comparable to that of a helium atom at very low T.

Gor'kov and Chernikova have studied the collective modes of the coupled electron–surface system in the high density limit (GC73). Two kinds of instability are predicted to occur as the surface deforms in order to minimize the Coulomb energy. One such deformation has a characteristic length of order the He capillary constant, $a_c = (2\sigma/\rho g)^{1/2} \approx 0.07$ cm. The associated instability appears when the electron density exceeds $n_1 = (\rho g\sigma)^{1/4}/(2\pi e^2)^{1/2} \approx 2 \times 10^9$ cm^{-2}. Another instability occurs for density greater than $n_2 = (\rho g h_e/6\pi e^2)^{1/2}$, where h_e is the surface height above the submerged electrode. If $h_e < 0.2$ cm, $n_2 < n_1$ and the second instability will appear first. Such densities can be obtained experimentally and the instabilities are of considerable interest.

IV. INTERNAL ELECTRONIC SURFACE STATES

Figure 2 depicts the geometry relevant to the internal electronic surface state. Electrons, produced in the liquid by a radioactive source or by cathode injection, localize in bubbles in about 10^{-12} sec (OnS71). Electrodes placed on either side of the liquid–vapor interface establish an electric field F which accelerates the electron bubbles toward the interface from below. This upward force is opposed by the image force, which is directed downward to maximize the attractive electron–He polarization interaction. The total potential energy of the bubble is

$$V(z) = -Q'e^2/z - Fez, \qquad z < 0, \tag{22}$$

$$Q' = Q/\epsilon.$$

This form of V is not valid close to the surface, because of finite bubble size and diffuseness of the liquid–vapor interface. $V(z)$ has a minimum at a distance $(-z_0) = (Q'e/F)^{1/2}$ from the surface. Near $z_0 =$ the potential is approximately harmonic with a force constant $k_0 = V''(z_0)$ given by

$$k_0 = 2(eF^3/Q')^{1/2}. \tag{23}$$

The motion of the bubble is characterized by an effective mass M which is of order two hundred times the mass of a single atom.[14] This determines the characteristic frequency in the potential [Eq. (22)],

$$\omega_0 = (k_0/M)^{1/2} \tag{24}$$

Another parameter of the bubble motion is $\langle\Delta z\rangle$, defined as two times the average amplitude of the classical oscillation at a temperature T. In the harmonic approximation one finds

$$\langle\Delta z\rangle = (8k_BT/k_0)^{1/2}.$$

The magnitude of $\langle\Delta z\rangle$ at $T = 1$ K is presented in Table II along with other parameters of the bubble motion. Note that Δz is comparable to z_0 for these fields, implying that the bubble is not well localized and that anharmonic terms are important.

A. Bubble dynamics

Following the suggestion of Shikin (Sh70), Poitrenaud and Williams performed a resonance experiment to study the surface bubble states (PW72). A radio frequency electric field is applied in the z direction, and the absorbed power measured as a function of static field F (Fig. 11). A resonance occurs when the rf field frequency $2\pi\nu$ equals ω_0 of Eq. (24). At the experimental temperature $T = 0.7$ K, the momentum relaxation time τ_m is $\approx 1.4 \times 10^{-8}$ sec (Sc72), so $\omega_0\tau_m > 1$ and the resonance is relatively sharp.

The effective mass M that results[15] is about 65 ^{4}He

TABLE II. Parameters of bubble oscillation at $T = 1$ K as a function of applied field F. An effective mass of 200 ^{4}He atomic masses has been assumed.

F(V/cm)	$\lvert z_0\rvert$(Å)	$\langle\Delta z\rangle$(Å)	$k_0(10^{-4}K/Å^2)$	$\omega_0(10^8$Hz)	$\hbar\omega_0/k_B(mK)$
50	434	548	0.27	1.66	1.27
300	178	143	3.91	6.37	4.86
600	126	85	11.05	10.71	6.17

[14] M is approximately equal to the classical hydrodynamic value of half the displaced liquid mass. For an excellent review of ions in liquid He, see (Fe74).

[15] The quantities M and R are revisions of those reported earlier (J. Poitrenaud, private communication).

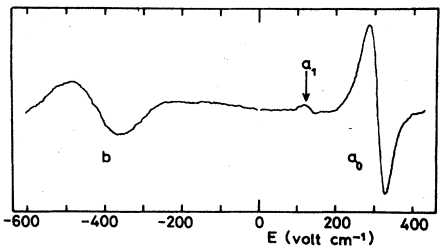

FIG. 11. Resonance absorption of (a) positive ions and (b) negative ions (bubble electrons) beneath the surface at $T = 0.7$ K. The rf frequency is fixed at $\nu = 209.4$ MHz and the static field varied. From (PW72).

masses, corresponding to a radius R of 10.9 ± 0.1 Å. These values are quite low relative to previously accepted ones (Fe74, PC74). However this experiment represents the most precise and direct determination of M to date, as no bulk cyclotron resonance measurement has succeeded. A momentum relaxation time measurement by Dahm and Sanders led to the conclusion that M falls in the interval 100–200 atomic masses (DS66, 70). One distinguishing feature of the surface experiment is the absence of liquid from the vapor half-space. Here M is determined by the kinetic energy of hydrodynamic flow about the bubble, which is proportional to $v^2(r) \approx r^{-6}$, where r is the distance from the bubble. Thus there is a mass shift $\delta M \propto -|z|^{-3}$ as the surface is approached. However this should be a small effect unless the bubble comes closer to the surface than about $2R$.

It should be noted in contrast that the positive ion studied in the same experiment yields a very reasonable effective mass ($\approx$44). A first harmonic for the positive appears in Fig. 11, suggesting the possibility that the single negative ion resonance observed is not the fundamental (Pa73). This would improve the situation considerably because it would imply $M \approx 250$ ($R \approx 17.5$ Å)—actually less when anharmonic corrections are made. Thus this is a plausible explanation, pending further data. [*Note added in proof:* New measurements confirm this hypothesis (J. Poitrenaud, to be published).]

While the resonance position is puzzling, the observed linewidth can be successfully explained. The equation of motion of the ion in the absence of the rf field is

$$M\ddot{\mathbf{r}} = -\nabla V(z) - \eta\dot{\mathbf{r}}, \tag{25}$$

where $\mathbf{r}$ is the ion position vector, and $V(z)$ given in (22) includes the static field. The drag coefficient η has the value e/μ, in which we can use the low field mobility μ for the complete velocity range of interest (SS68, Sc72). One can easily calculate the power absorbed from an rf field of frequency ν, if V is assumed to be harmonic, a restriction we relax below. The peak-to-minimum width in the derivative curve is then predicted to be $\Delta\nu = \eta/(\sqrt{3}2\pi M)$. Converting this to a static field width ΔF through the relation $\omega_0 \propto F^{3/4}$ from Eqs. (23) and (24) yields

$$\Delta F/F = 2/(3^{3/2}\pi\tau\nu). \tag{26}$$

For the case $\nu \approx 2.09 \times 10^8$ Hz, $F \approx 398$ V/cm, one finds $\Delta F \approx 16$ V/cm, which is small compared to the observed width of 90 V/cm (PW72). The discrepancy is due to anharmonicity of the potential $V(z)$, which can be shown to dominate the broadening. Expanding the potential about z_0, we have

$$\begin{aligned} V(z) &= V(z_0) + k_0(z - z_0)^2/2 + c_3(z - z_0)^3 \\ &\quad + c_4(z - z_0)^4 + \cdots, \qquad (27) \\ c_3 &= Q'e^2/z_0^4, \\ c_4 &= -Q'e^2/z_0^5. \end{aligned}$$

If terms in V beyond quartic are neglected, the eigenvalues of the Schrödinger equation can be determined (LaL58). The energy separation between levels j and $j - 1$, equivalent in the large j limit to the classical frequency times h, is

$$\Delta E_j = \hbar(\omega_0 - j\omega_1),$$

where

$$\omega_1 = 15c_3^2\hbar/2m^3\omega_0^4 - 3c_4\hbar/m^2\omega_0^2. \tag{28}$$

Assuming the thermal distribution of oscillators among levels to be approximately proportional to $\exp(-j\beta\hbar\omega_0)$, one finds a distribution of absorption frequencies

$$f(\omega) \propto \exp[-\beta\hbar\omega_0(\omega_0 - \omega)/\omega_1], \qquad \omega < \omega_0.$$

This determines a width in the absorption line due to anharmonicity

$$\begin{aligned} (\Delta\omega)_{an} &= \ln 2(\omega_1/\beta\hbar\omega_0) \\ &= (27 \ln 2/2^{7/2}) k_B T (F/M^2Q'^3e^5)^{1/4}, \qquad (29) \end{aligned}$$

where the values of z_0 and ω_0 have been substituted in Eqs. (27) and (28). The width in F that follows from this expression is $(\Delta F)_{an} \approx 64$ V/cm, which is four times as large as the momentum relaxation linewidth and determines a total of order 80 V/cm, in good agreement with the observed 90 V/cm. Furthermore the linear T dependence of Eq. (29) and magnitude of ΔF for the positive ion agree with experiment.

Poitrenaud and Williams report some dependence on ion density of the linewidth for negative ions, but none for positive ions. We estimate the effect of interactions as follows. Consider two bubbles constrained to oscillate on lines perpendicular to the surface which are separated by a distance D. If the z component of the separation, $\Delta z = z_2 - z_1$, is much smaller than D, the z component of the force between them is $e^2\Delta z/\epsilon D^3$. The out-of-phase normal mode frequency of their coupled motion then differs from ω_0 by $\delta\omega_0 = -e^2/\epsilon D^3 M\omega_0$. Because D varies, the absorption line is broadened by a corresponding $(\Delta F)_c \approx 0.01$ V/cm for a density 3×10^7 cm^{-2}. This value is small relative to other contributions to the broadening. The existing data is inadequate to make a comparison with this estimate.

Another experiment suggested by Shikin is a mobility measurement with a field component parallel to the surface (Sh70). The mobility will differ from the bulk value because the dominant scatterers at low T, phonons and ^{3}He atoms, satisfy boundary conditions at the surface, and also because ripplons will contribute there. Shikin calculated the phonon-limited mobility, considering effects of the boundary conditions at both the free surface and the bubble surface. Taking

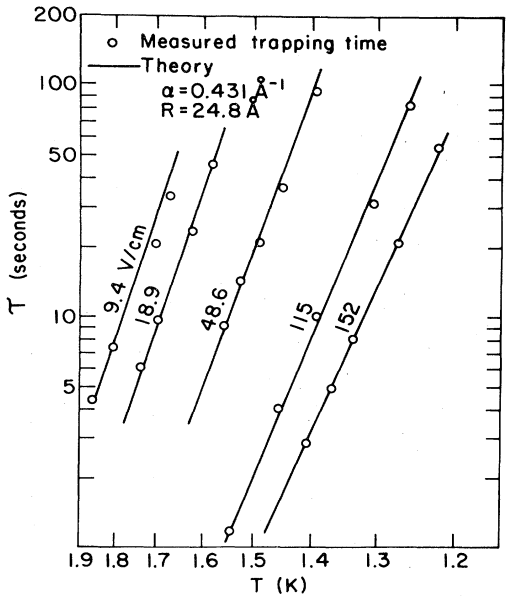

FIG. 12. Measurements of trapping time of electrons in bubbles beneath the surface as a function of applied field and temperature. The solid lines are calculated by Schoepe and Rayfield (SR73) using the radius and decay constant values shown.

the pressure excursion due to the phonon as vanishing at the interface implies a decreased scattering of bubbles located at $z \lesssim \lambda_p$, the phonon wavelength. As T decreases, the characteristic phonon wavelength increases as T^{-1}, so the region of reduced scattering moves outward from the interface. Thus the surface mobility rises above the bulk when the condition $z_0 \lesssim hc\beta$ is satisfied, where c is the speed of sound.

The contribution of ripplon scattering should become important for z small compared to a thermal ripplon wavelength $\lambda_r \approx 2\pi[\sigma\hbar^2\beta^2/\rho]^{1/3}$. At $T = 0.7$ K, for example, $\lambda_r \approx 40$ Å, compared to $\lambda_p \approx 160$ Å. These effects should be further explored.

B. Field emission from bubbles

Several experiments have investigated field emission of electrons from bubbles (CFG60, BMM66, ScP70, RS71a, RS71b, SR73, CW72). Recently Schoepe and Rayfield performed a detailed analysis which successfully explains their trapping time data in terms of tunneling of the electron from bubble to vapor, through the liquid potential barrier V_0 (SR73).[16]

The experiment measures a current j arriving at an electrometer above the surface, as a function of time after an initial number of electrons in bubbles are positioned beneath the surface. The current is observed to decay exponentially with a characteristic time τ of order 1–100 seconds (see Fig. 12). This time is long compared to that required for the bubbles to equilibrate ($\approx 10^{-10}$ sec) with the He. It is therefore plausible that their distribution in space $n(z)$ corresponds to equilibrium in the absence of the emission process. At high temperature ($\beta\hbar\omega_0 \ll 1$), $n(z)$ can be taken to have Maxwell–Boltzmann form corresponding to the Brownian motion of the heavy ion,

$$n(z) = c \exp[-\beta V(z)], \tag{30}$$

where c normalizes the integral of $n(z)$ over z to give the instantaneous number of electrons present in the liquid. If one knows $t(z)$, the probability per unit time of tunneling from a bubble at z to the vapor, then one can obtain the total current leaving the liquid

$$j = e\int_{-\infty}^{-R} dz\, n(z)t(z). \tag{31}$$

Schoepe and Rayfield use a semiclassical Ansatz for $t(z)$. If an electron's tunneling trajectory is inclined at an angle θ to the surface normal, the path length in liquid is

$$l(\theta, z) = z/\cos\theta - R,$$

where R is the bubble radius. The probability for such an event can be estimated as the product of an attempt frequency $\nu_a \approx (2E_0/m)^{1/2}/2R$ in the bubble and a barrier penetration factor $\exp(-2\alpha l)$, where E_0 is the electron energy (≈ 0.1 eV) and

$$\alpha^2 = 2m(V_0 - E_0)/\hbar^2.$$

The total escape rate is obtained by integrating over $\theta < \pi/2$,

$$t(z) = \nu_a \iint_{\theta=0}^{\pi/2} \exp[-2\alpha l(\theta, z)]\, d\Omega/4\pi.$$

Since we know $V(z)$ and have reasonably accurate values for V_0 and R, the theory makes an unambiguous prediction for the field and T-dependent current j, or equivalently the decay constant τ. Conversely, we can use the experimental data to select best values for V_0 and R. The latter procedure has been used in Fig. 12 to yield excellent agreement with $V_0 \approx 0.82$ eV and $R = 24.8$ A. This result for V_0 is consistent with, although somewhat smaller than, previous values (see Sec. II). However $R = 24.8$ A is considerably higher than the current best estimate of 16 A. As noted by (SR73), this could arise from a missing constant factor[17] in the expression for j, since R enters primarily through a factor $\exp(2\alpha R)$. It is conceivable that a better calculation of $t(z)$ will remedy this discrepancy. Such a calculation would have to incorporate inelastic processes involving bubble relaxation during tunneling. [*Note added in proof:* A tunneling Hamiltonian calculation by the author, to be published, finds an even smaller $t(z)$, hence even larger value of R.]

Because $t(z)$ falls off exponentially with z, prediction of the current is quite sensitive to assumptions about both the bubble surface and the liquid–vapor interface, even

[16] Williams and Crandall (WC71b) and Springett (Sp72) have shown how the early DC current measurements can be related to trapping times.

[17] Since $\alpha \approx 0.43$ Å^{-1}, the constant is about 2000. This argument is especially appealing because a comparable factor is needed for the ^{3}He case.

though the *mean* bubble position is far from the surface. If $F = 150$ V/cm, for example, most of the emission comes from bubbles about 33 Å from the surface (SR73), even though $z_0 \approx 250$ Å. These electrons tunnel through a barrier about 5 interatomic spacings wide. The diffuseness of each of the two surfaces penetrated is about one interatomic spacing (Co70a, ShW73, PC74), so this represents an important consideration (KRK70).

Recently considerable attention has been focused on the nature of the electronic states in dense He vapor, especially in the vicinity of the localized free transition (EC70, 71, Eg72, He73) mentioned above. Tunneling from bubble to vapor is capable of probing the energy spectrum of both initial and final states. In particular, the electron energy in the bubble, E_0, decreases with T, becoming equal to the minimum energy in the vapor $V_0(n_V)$ at about 4.2 K. If the electron tunnels elastically, one would expect a rapid decrease in the rate near this temperature. However, preliminary results of Schoepe and Wagner in the range 3–4.6 K show a relatively slow decrease with temperature (ScW73). Further investigation of this aspect will be quite valuable.

We mention for completeness that several experiments have explored emission of electrons from negatively charged vortex rings accelerated toward the surface (CDMR68, SuR68, MR72, HSp72). This differs from the bubble problem in that the vortex ring interaction with the surface is the dominant effect. If the interface remains flat, an approaching ring expands and slows down, eventually permitting the electron to tunnel from about 50 Å below the interface (HSp72).

V. CONCLUSION

Our understanding of each species of surface state stands at an intermediate stage of development. While experiment has confirmed the basic ideas, several important questions remain. Some of these are listed below.

We lack experimental demonstration of the electron–ripplon interaction for the external state. This may result from an extension of existing experiments to temperatures below 1 K. Equally interesting would be a manifestation of electron localization, either in a Wigner lattice or in single-particle states near a surface depression. Both theoretical and experimental work would be valuable.

For the internal state we need an explanation for the large effective mass deviation from the bulk values. Improved calculations of the surface modification of the tunneling rate are necessary in order to learn about diffuseness of both the bubble surface and the liquid–vapor interface. Mobility experiments will be useful for these states as well.

ACKNOWLEDGMENTS

It is a pleasure to thank T. Brown, M. H. Cohen, R. S. Crandall, J. G. Dash, C. C. Grimes, J. Herb, T. C. Padmore, R. D. Puff, M. Schick, W. Schoepe, J. R. Schrieffer, and L. Sander for helpful discussion and other assistance. I am grateful in particular to P. Berdahl and K. Schwarz for many suggestions for improving the paper.

REFERENCES

An65 H. A. Antosiewicz, in *Handbook of Mathematical Functions*, edited by M. Abramowitz and I. A. Stegun (Dover, N.Y., 1965), Sec. 10.4.

BD66 D. J. BenDaniel and C. B. Duke, Phys. Rev. **152,** 683 (1966).

BD67 D. J. Ben Daniel and C. B. Duke, Phys. Rev. **168,** 832 (1967).

BG72 T. R. Brown and C. C. Grimes, Phys. Rev. Lett. **29,** 1233 (1972).

BMM66 L. Bruschi, B. Maraviglia, and F. Moss, Phys. Rev. Lett. **17,** 682 (1966).

Bu65 B. Burdick, Phys. Rev. Lett. **14,** 11 (1965).

CC69 M. W. Cole and M. H. Cohen, Phys. Rev. Lett. **23,** 1238 (1969).

CDMR68 S. Cunsolo, G. Dall'oglio, B. Maraviglia, and M. V. Ricci, Phys. Rev. Rev. Lett. **21,** 74 (1968).

CFG60 G. Careri, U. Fasoli and F. S. Gaeta, Nuovo Cimento **15,** 774 (1960).

CGHM71 D. G. Castello, D. E. Groce, D. F. Herring and J. W. McGowan, Phys. Rev. B **5,** 1433 (1971).

Ch71 A. V. Chaplik, Zh. Eksp. Teor. Fiz. **62,** 746 (1971) [Sov. Phys.—JETP **35,** 395 (1971)].

Co70a M. W. Cole, Phys. Rev. A **1,** 1838 (1970).

Co70b M. W. Cole, Phys. Rev. B **2,** 4239 (1970).

Co71 M. W. Cole, Phys. Rev. B **3,** 4418 (1971).

Cr72 R. S. Crandall, Phys. Rev. A **6,** 790 (1972).

Cr73 R. S. Crandall, Phys. Rev. A **9,** 2136 (1973).

Cr74 R. S. Crandall, Phys. Rev. A, to be published, 1974.

CW71 R. S. Crandall and R. Williams, Phys. Lett. A **34,** 404 (1971).

CW72 R. S. Crandall and R. Williams, Phys. Rev. A **5,** 2183 (1972).

DB72 J. G. Dash and M. Bretz, J. Low Temp. Phys. **9,** 291 (1972).

DS66 A. J. Dahm and T. M. Sanders, Jr., Phys. Rev. Lett. **17,** 126 (1966).

DS70 A. J. Dahm and T. M. Sanders, Jr., J. Low Temp. Phys. **2,** 199 (1970).

Du68 C. B. Duke, Phys. Rev. **168,** 816 (1968).

EC70 T. P. Eggarter and M. H. Cohen, Phys. Rev. Lett. **25,** 807 (1970).

EC71 T. P. Eggarter and M. H. Cohen, Phys. Rev. Lett. **27,** 129 (1971).

Eg72 T. P. Eggarter, Phys. Rev. A **5,** 2496 (1972).

ElG73 R. L. Elgin and D. L. Goodstein, in *Monolayer and Submonolayer Helium Films*, edited by J. G. Daunt and E. Lerner (Plenum, N.Y., 1973); and to be published.

EM72 E. Evans and D. L. Mills, Solid State Commun. **11,** 1093 (1972).

EM73 E. Evans and D. L. Mills, Phys. Rev. B **7,** 853 (1973).

F24 E. Fermi, Z. Phys. **26,** 54 (1924).

Fe74 A. L. Fetter in *The Physics of Liquid and Solid Helium*, edited by K. H. Bennemann and J. B. Ketterson (Wiley, N.Y., 1974).

GB74 C. C. Grimes and T. R. Brown, Phys. Rev. Lett. **32,** 280 (1974).

GC73 L. P. Gor'kov and D. M. Chernikova, Zh. Eksp. Teor. Fiz Pis'ma Red **18,** 119 (1973) [JETP Lett. **18,** 68 (1973).

GR65 I. S. Gradshteyn and I. M. Ryzhik, *Table of Integrals, Series and Products*, (Academic, N.Y., 1965), 4th edition.

He73 J. P. Hernandez, Phys. Rev. A **7,** 1755 (1973).

HS73 C. H. Hodges and M. J. Stott, Solid State Commun. **12,** 1153 (1973).

HSp72 C. Hosticka and B. E. Springett, Phys. Rev. A **6,** 492 (1972).

JK70 J. Jortner and N. R. Kestner, J. Pure Appl. Chem. (Metal Ammonia Solutions Suppl.) **5** (1970).

JKRC65 J. Jortner, N. R. Kestner, S. A. Rice, and M. H. Cohen J. Chem. Phys. **43,** 2614 (1965).

KJCR65 N. R. Kestner, J. Jortner, M. H. Cohen, and S. A. Rice Phys. Rev. **140,** A56 (1965).

KRK70 M. Kuchnir, P. R. Roach, and J. B. Ketterson, J. Low Temp. Phys. **3,** 183 (1970).

KT72 J. M. Kosterlitz and D. J. Thouless, J. Phys. C **5,** L124 (1972).

KT73 J. M. Kosterlitz and D. J. Thouless, J. Phys. C **6,** 1181 (1973).
LaL58 L. D. Landau and E. M. Liftshitz, *Quantum Mechanics* (Pergamon Press, London, 1958), p. 136.
Ll67 P. Lloyd, Proc. Phys. Soc. Lond. **90,** 207 (1967).
LS67 J. L. Levine and T. M. Sanders, Jr., Phys. Rev. **154,** 138 (1967).
M46 H. J. Margenau, Phys. Rev. **69,** 508 (1946).
MD70 T. Miyakawa and D. L. Dexter, Phys. Rev. A **1,** 1513 (1970).
ME68 N. D. Mermin, Phys. Rev. **176,** 250 (1968).
MR72 R. P. Mitchell and G. W. Rayfield, Phys. Lett A **42,** 267 (1972).
MS70 H. J. Mikeska and H. Schmidt, J. Low Temp. Phys. **2,** 371 (1970).
O73 R. M. Ostermeier, private communication.
OnS71 D. G. Onn and M. Silver, Phys. Rev. A **3,** 1773 (1971).
OS72 R. M. Ostermeier and K. W. Schwarz, Phys. Rev. Lett. **29,** 25 (1972).
Pa73 T. C. Padmore, private communication, 1973.
PC74 T. C. Padmore and M. W. Cole, Phys. Rev. A **9,** 802 (1974).
PW72 J. Poitrenaud and F. I. B. Williams, Phys. Rev. Lett. **29,** 1230 (1972).
PW73 J. Poitrenand and F. I. B. Williams, private communication, 1973.
RS71a G. W. Rayfield and W. Schoepe, Phys. Lett. A **31,** 133 (1971).
RS71b G. W. Rayfield and W. Schoepe, Z. Naturforsch. A **26,** 1392 (1971).
S71 W. F. Saam, Phys. Rev. A **4,** 1278 (1971).
Sa72 J. Sak, Phys. Rev. B **6,** 3981 (1972).
Sc72 K. W. Schwarz, Phys. Rev. A **6,** 837 (1972).
ScP70 W. Schoepe and C. Probst, Phys. Lett. A **31,** 490 (1970).
ScW73 W. Schoepe and F. Wagner, preprint, 1973
Sh70 V. B. Shikin, Zh. Eksp. Teor. Fiz. **58,** 1748 (1970) [Sov. Phys.—JETP **31,** 936 (1970)];
Sh71a V. B. Shikin, Zh. Eksp. Teor. Fiz. **60,** 713 (1971) [Sov. Phys.—JETP **33,** 387 (1971)].
Sh71b V. B. Shikin, Zh. Eksp. Teor. Fiz. **61,** 2053 (1971) [Sov. Phys.—JETP **34,** 1095 (1972)].
Sho39 W. Shockley, Phys. Rev. **56,** 317 (1939).
ShW73 Y. M. Shih and C.-W. Woo, Phys. Rev. Lett. **30,** 478 (1973).
SJC68 B. E. Springett, J. Jortner, and M. H. Cohen, J. Chem. Phys. **48,** 2720 (1968).
So64a W. T. Sommer, Phys. Rev. Lett. **12,** 271 (1964).
So64b W. T. Sommer, Thesis, Stanford University, 1964, (unpublished).
Sp72 B. E. Springett, Phys. Rev. A **5,** 2666 (1972).
SR73 W. Schoepe and G. W. Rayfield, Phys. Rev. A **7,** 2111 (1973).
SS68 K. W. Schwarz and R. W. Stark, Phys. Rev. Lett. **21,** 967 (1968).
ST71 W. T. Sommer and D. J. Tanner, Phys. Rev. Lett. **27,** 1845 (1971).
SuR68 C. M. Surko and F. Reif, Phys. Rev. **175,** 229 (1968).
Ta73 L. L. Tankersley, J. Low Temp. Phys. **11,** 451 (1973).
WC71a R. Williams and R. S. Crandall, Phys. Lett. A **36,** 35 (1971).
WC71b R. Williams and R. S. Crandall, Phys. Rev. A **4,** 2024 (1971).
WCW71 R. Williams, R. S. Crandall, and A. H. Willis, Phys. Rev. Lett. **26,** 7 (1971).
WW63 E. T. Whittaker and G. N. Watson, *A Course of Modern Analysis* (Cambridge University Press, 1963), Sec. 16.
Zi67 J. Ziman, Proc. Phys. Soc. Lond. **91,** 701 (1967).
ZS68 C. Zipfel and T. M. Sanders, Jr., in *Proc. XI International Conference on Low Temperature Physics, 1968,* edited by J. F. Allen, D. M. Finlayson, and D. M. McCall (St. Andrews, Scotland, 1969), p. 296.

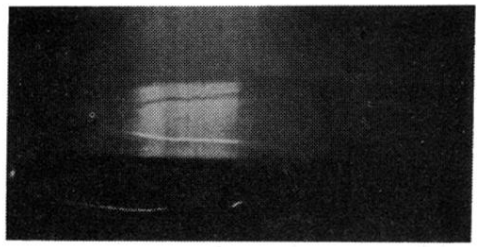

(b)

FIG. 10. Depression of a liquid He surface due to the presence of 2.5×10 electrons/cm^2. The applied field is 2000 V/cm. The depth of the depression is about 0.1 mm. From (WC71a).